·实验研究·

载槲皮素 PNIPAm 纳米凝胶的制备及细胞学研究

吕方南[1]，黄洁[1]，陈剑秋[1]，赵子明[1,2]，金超颖[1]，杜倩[1,2]
(1.徐州医科大学药学院，江苏 徐州 221004；2.江苏省新药研究与临床药学重点实验室，江苏 徐州 221004)

摘要：目的 以聚(N-异丙基丙烯酰胺)(PNIPAm)凝胶为纳米载体，荷载抗肿瘤成分槲皮素，以增加药物对 MCF-7 细胞的毒性和细胞摄取。**方法** 采用正交设计优化 PNIPAm 合成工艺，红外光谱进行结构确证；单因素试验优化载槲皮素纳米凝胶(Que-PNIPAm)处方及工艺，分别对粒径、表面形态、载药量进行表征并考察体外释放行为；CCK-8 法考察纳米凝胶对 MCF-7 细胞的毒性；荧光倒置显微镜和流式细胞仪对纳米凝胶的 MCF-7 细胞摄取作用进行定性观察和定量测定；抑制剂法考察其细胞摄取机制。**结果** Que-PNIPAm 的粒径为(166.1±2.87) nm，载药量为 3.18%；电镜下纳米粒子呈类球形、粒径分布均匀；载药纳米凝胶对 MCF-7 细胞的抑制作用显著高于原药，且 42℃下显示出更高的细胞摄取效率和抑制肿瘤细胞增殖活性；秋水仙素与 2-去氧葡萄糖对细胞摄取有抑制作用。**结论** 制备的载药纳米凝胶粒径小，具有温敏特性，能够显著增强药物被细胞摄取能力及肿瘤细胞毒性，MCF-7 细胞对 PNIPAm 的摄取机制为微管蛋白途径。

关键词：MCF-7 细胞；PNIPAm 纳米凝胶；槲皮素；细胞毒性；细胞摄取
中图分类号：R283.6 **文献标志码：**A **文章编号：**1672－0482(2020)02－0197－08
DOI：10.14148/j.issn.1672-0482.2020.0197
引文格式：吕方南，黄洁，陈剑秋，等.载槲皮素 PNIPAm 纳米凝胶的制备及细胞学研究[J].南京中医药大学学报，2020，36(2)：197-204.

Development and Cytological Study of PNIPAm-Based Nanogels Loaded with Quercetin

***LYU Fang-nan*[1], *HUANG Jie*[1], *CHEN Jian-qiu*[1], *ZHAO Zi-ming*[1,2], *JIN Chao-ying*[1], *DU Qian*[1,2]**
(1. School of Pharmacy, Xuzhou Medical University, Xuzhou, 221004, China; 2. Jiangsu Key Laboratory of New Drug Research and Clinical Pharmacy, Xuzhou, 221004, China)

ABSTRACT: OBJECTIVE To improve uptake and cytotoxicity of the drug on MCF-7 cells by developing a poly (*N*-isopropylacrylamide) (PNIPAm) nanogel for Quercetin (Que) **METHODS** The PNIPAm nanogel was optimized by an orthogonal design and its structure was confirmed by FT-IR. A single factor experiment was used to optimize the formulation of quercetin-loaded nanogel (Que-PNIPAm). The particle size, surface morphology and drug loading were characterized and the *in vitro* release behavior was investigated. Cytotoxicity of MCF-7 cells induced by Que-PNIPAm was investigated by CCK-8 method. The qualitative and quantitative cellular uptake studies were investigated by fluorescence microscope and flow cytometry, respectively. The mechanism of cellular uptake was investigated by the inhibitor method. **RESULTS** The particle size and drug loading of Que-PNIPAm were measured as (166.1±2.87)nm and 3.18%, respectively. Nanogel exhibited spherical morphology and uniform size distribution observed by electron microscopy. Compared to free Que, Que-PNIPAm significantly increased inhibition rate of MCF-7 cells. Que-PNIPAm also showed higher cell uptake efficiency and more effective antitumor activity at 42 ℃. Colchicine and 2-deoxyglucose have an inhibitory effect on MCF-7 cells uptake. **CONCLUSION** The prepared nanogel shows small particle size, thermosensitive property, which could significantly enhance the capacity of cellular uptake and tumor cytotoxicity. The mechanism of cellular uptake demonstrates tubulin is involved in the internalization of the nanogel into MCF-7 cells.

KEYWORDS: MCF-7 cells; PNIPAm nanogel; quercetin; cytotoxicity; cellular uptake

Quercetin (3,3′,4′,5,7-pentahydroxyflavone, Que) is an abundant flavonoid in medical plants, including *Ginkgo biloba L.*, *Apocynum lancifolium Rus.*, *Tussilago farfara L.*, *Sophora japonica L.* and *Hippophae rhamnoides L* [1-3]. Que possesses a broad spectrum of anticancer activity [4-5]. Still, the potential of Que has not been sufficiently exploited, partly due to the low water solubility (0.7－7.7 μg/mL) and poor cellular uptake [6-8]. To resolve these physicochemical limitations, a variety of biodegradable nanocarriers for Que delivery have been developed, which

收稿日期： 2019-11-19
基金项目： 国家自然科学基金(81603302，81773643)；江苏省自然科学基金(BK20150215)
第一作者： 吕方南，男，硕士研究生，E-mail：lvfangnan@126.com
通信作者： 杜倩，女，副教授，主要从事中药新制剂研究，E-mail：duqian81@126.com

based on liposomes, micelles, lipid nanoparticles and polymers [9-10]. Amidst various nanocarriers, stimuli-responsive polymers have gained much attention due to the ability of phase transition in response to external environment changes, such as light, electric field strength, temperature *etc* [11-14]. Therein, poly (N-isopropylacrylamide) (PNIPAm) has been widely reported as a thermosensitive polymer for biomedical applications. It has been shown that water-soluble PNIPAm has better available efficacies of temperature-modulated cellular uptake due to its contract-stretch chain changes across the lower critical solution temperature (LCST) [15-16].

In view of this, we have considered that the use of PNIPAm could be an effective pathway to enhance cellular uptake and toxicity of the hydrophobic Que on MCF-7 breast cancer cells. In our study, as shown in Figure 1, PNIPAm was obtained through emulsion polymerization by means of orthogonal design, and Que-PNIPAm was prepared by single factor experiment for higher drug loading. *In vitro* characterizations, MCF-7 cell uptake efficiency, cytotoxicity of the nanocarriers were conducted, including evaluation of the temperature-responsive properties. Additionally, MCF-7 cell uptake mechanism was further investigated by flow cytometry with using various inhibitors.

1 Materials and methods

1.1 Reagents and drugs

Quercetin (Que) was purchased from Pufeide Biotech Co. Ltd. (Chengdu, China). Ammonium persulfate (APS), Methylene-bis-acrylamide (MBA), Dimethyl sulfoxide (DMSO) were purchased from Sinopharm Chemical Reagent Co. Ltd. (Shanghai, China). Lauryl sodium sulfate (SDS) was purchased from Usolf Bio-Technology Co. Ltd. (Shandong, China). *N*-isopropylacrylamide (NIPAm) was purchased from Energy Chemical Co. Ltd. (Shanghai, China). Colchicine and 2-deoxy-D-glucose were purchased from Yuanye Bio-Technology Co. Ltd. (Shanghai, China). Coumarin-6, Nystatin and Ammonium chloride were purchased from Aladdin Bio-Chem Technology Co. Ltd. (Shanghai, China). Chloroquine was purchased from Ark Pharm Co. Ltd. (Shanghai, China). Fetal bovine serum (FBS) was purchased from Clark bioscience Co. Ltd. (Virginia, America). Cell Counting Kit-8 (CCK-8) was purchased from Beyotime Bio-Technology Co. Ltd. (Shanghai, China). Trypsin-EDTA, Dulbecco's Modified Eagle Medium (DMEM) and non-essential amino acid were purchased from Keygen Bio-Technology Co. Ltd. (Jiangsu, China). 0.9% sodium chloride injection was purchased from Hualu Pharmaceutical Co. Ltd. (Shandong, China). Formic acid and methanol were of chromatographic grade. The water used in all experiment was ultrapure water. All other reagents are of analytical grade.

1.2 Preparation of PNIPAm Nanogel

An emulsion polymerization method was used to prepare the PNIPAm nanogel [17-18]. Surfactant SDS (22.6 mg) and cross-linking agent MBA were weighed into a flask and dissolved in deionized water. The system was protected by use of nitrogen. The PNIPAm monomer (4 mmol) and initiator APS were added respectively and mixed by use of a magnetic stir bar at a preset temperature. Following the reaction, the product was treated by use of an ultrasonic cell processor and dialyzed in water for 24 h, with water changes every 12 h. Next, the PNIPAm nanogel was obtained by lyophilization.

1.3 Orthogonal Design

Concentrations of MBA and APS, reaction time and temperature were optimized in the production of the PNIPAm nanogel. As presented in Table 1, each factor was assessed at three levels. Particle size is a key factor for judging the process of polymerization reaction and influencing cellular internalization of nano-carriers. Therefore, particle size measured at various temperatures were taken as the evaluating index [19-20]. The optimal factors were selected through intuitive and variance analysis [21-22].

1.4 Fourier transform infrared spectroscopy (FT-IR)

A FT-IR spectrometer (FTIR-8400s, SHIMADZU, Japan) was used to monitor spectras of NIPAm monomer and PNIPAm nanogel at a wavelength between 400～5 000 cm^{-1}. To prepare flakes, samples were mixed with KBr and compressed by a tablet press to produce discs with a diameter equal to 10 mm.

1.5 Scanning electron microscopy (SEM)

Surface morphology of PNIPAm nanogel was observed using a SEM (TENEO VS, FEI, USA). The lyophilized formulation was coated with gold under vacuum and characterized at an accelerating voltage of 10 kV.

1.6 Drug loading

Que-PNIPAm nanogel was prepared by use of an incubation method under aqueous conditions. PNIPAm nanogel lyophilized product was added to milli-Q water and sonicated until the system was completely dissolved. Excess Que was dissolved in a mixed ethanol and acetone solution (1∶1, v/v), then added into the nanogel solution with magnetic stirring at 400 r/min until complete mixing. Next, the system was incubated at a preset temperature and protected from light for 12 h. To investigate the effect of each parameter on drug loading, the formulation was determined by a single factor experiment, using incubation temperature (4 ℃, 25 ℃ and 37 ℃), ratio of Que and PNIPAm (1∶5, 1∶10 and 1∶20) and PNIPAm concentration (10 mg/mL, 20 mg/mL, 30 mg/mL, 50 mg/mL and 80 mg/mL). Unloaded Que was removed by 5 min of centrifugation at 2 000 r/min, the supernatant was passed through a 0.45 μm filter and the filtrate was diluted with methanol. The HPLC method was used to assess drug loading and calculated as:

$$\text{Drug loading}=\frac{\text{Mass of Our in PNIPAm nanogel}}{\text{Mass of total Our-PNIPAm nanogel used}}\times 100\%$$

1.7 HPLC method

An HPLC method was used to determine the amount of Que in the preparation by use of a C_{18} column (Wondasil C_{18}-WR, 4.6 mm × 250 mm, 5 μm). The isocratic mobile phase was a mixture of methanol and 0.1% formic acid (v/v = 65∶35) and delivered at a flow rate of 1 mL/min and at 30 ℃. A standard curve for Que concentration in methanol was used for quantification purpose. Que was mo-

nitored at 360 nm, an injection volume of 20 μL and in the retention window of 6 min. The linearity range of the method was 1－20 μg/mL (R^2 = 0.999 4). Que reference solutions were prepared at three different concentrations, injected five times to calculate intra-day precision. Each concentration of Que was continuously measured for 3 days to calculate inter-day precision. Results are presented as percentage relative SD, intra-day precision was 0.95%, 0.51% and 2.49% (n=5), and inter-day precision was 1.62%, 2.64% and 2.68% (n = 3), respectively. Rates of recovery for the method were 96.40%, 97.00% and 101.00%.

1.8　Transmission electron microscope (TEM)

The morphology of the Que-PNIPAm nanogel was visualized by use of TEM (TECNAI G2 Spirit Twin, FEI, USA). The prepared Que-PNIPAm solution was dropped onto a carbon-coated copper grid with 300-mesh and dried. TEM photos of Que-PNIPAm were observed at an accelerating voltage of 200 kV at different magnifications.

1.9　*In vitro* drug release

In vitro release of free Que and Que-PNIPAm nanogel were investigated using the dialysis method [23]. 1 mL of drug-loaded nanogel was sealed in each dialysis bag (MW: 1 000 kDa). Dialysis bags were incubated in 80 mL of 35% ethanol solution with constant stirring at 100 r/min [24-25] and maintained at 37 ℃ and 42 ℃ in order to reflect the thermosensitive characteristics of the nanogel. 1 mL of each sample was collected at preset interval time and replaced with 1 mL fresh 35% ethanol solution. Each sample was filtered with a membrane filter (0.45 μm, Shimadzu, Japan) and 0.5 mL of the initial filtrate was removed. Next, remaining filtrate was collected for HPLC analysis. Measurements for rate of release were performed in triplicate. *In vitro* release of free Que was investigated for comparison with the nanogel.

1.10　Cell culture studies

Human breast cancer cells (MCF-7) were cultured in DMEM complemented with 10% FBS and 1% non-essential amino acid. Cells were incubated at 37 ℃ under atmosphere comprising 5% carbon dioxide (CO_2) [26]. The medium was replaced every 24 h before the cells were passaged.

1.11　Cytotoxicity

Cytotoxicity experiments were designed to investigate the impact of PNIPAm nanogel for Que delivery. Experiments were carried out using MCF-7 cells and cytotoxicity was assessed by the Cell Counting Kit-8 (CCK-8) assay [27]. Cells were seeded into 96-well plate at a density of 8×10^3 cells per well and incubated in a 5% CO_2 atmosphere at 37 ℃. After cells were incubated overnight for attachment, different concentrations of Que-PNIPAm nanogel and free Que solution were added (100 μL), cells in DMEM only (without drug and PNIPAm nanogel) were used as the control for comparison, cells were first incubated at different temperature (37 ℃ and 42 ℃) for 1 h and then followed by a 23 h incubation at 37 ℃. After 24 h cells were washed with 0.9% aqueous sodium chloride, 10% CCK-8 solution was added and cells were stored in the dark and incubated for 1 h. Next, absorbance was measured at 450 nm by use of a microplate reader (Varioskan LUX, Thermo Fisher SCIENTIFIC, USA). Results were presented as percentage of inhibition.

1.12　Cellular uptake

To assess the cellular uptake of the nanogel by MCF-7 cells, qualitative and quantitative studies were performed using Coumarin-6 (C6) as a fluorescence probe. Coumarin-6 was loaded in the PNIPAm nanogel according to the previously described preparation method for the Que-PNIPAm nanogel. After probe loading, no changes in nanogel characteristics were observed.

For qualitative study, MCF-7 cells were seeded into 24-well plate at a density of 1×10^4 cells per well and incubated in a 5% CO_2 atmosphere at 37 ℃ for 24 h. The prepared C6-PNIPAm nanogel was diluted with DMEM at various concentrations (75, 150 μg/mL or 300 μg/mL) and added to each well. In addition, PNIPAm nanogel (without C6) and free C6 solution were used as controls. Following exposure, cells were fixed with 4% paraformaldehyde for 10 min after incubation for 2 h in the dark, and then washed with 0.9% aqueous sodium chloride 5 times. Cells were observed by use of fluorescence microscopy (IX-73, Olympus, Japan) at excitation and emission wavelengths of 466 and 504 nm. The temperature-dependent cellular uptake properties of 1 h at 37 ℃ and 42 ℃ were also investigated under the same procedure.

For quantitative study, MCF-7 cells were seeded into 6-well plates at a density of 1×10^5 cells per well and incubated in a 5% CO_2 atmosphere at 37 ℃ for 24 h. The unloaded PNIPAm nanogel, free C6 solution and prepared C6-PNIPAm nanogel with different concentrations (75 μg/mL, 150 μg/mL or 300 μg/mL) were added to the appropriate well. After incubation at 37 ℃ for 2 h in the dark, cells were digested by use of 0.25% trypsin-EDTA and centrifuged at 1 000 r/min for 3 min. The supernatant was collected and cells resuspended in 0.9% aqueous sodium chloride. Effect of incubation time was also investigated, the prepared C6-PNIPAm nanogel was diluted with DMEM at a concentration of 150 μg/mL and incubated at 37 ℃ for different times in the dark (1 h, 2 h or 4 h). After digestion and centrifugation steps, the percentage of fluorescing cells was assessed by use of flow cytometry (Facs Canto Ⅱ, Becton, Dickinson and Company, USA).

Mechanisms of cellular uptake were further assessed using MCF-7 cells seeded on 6-well plates at a density of 1×10^5 cells per well and incubated in a 5% CO_2 atmosphere at 37 ℃ for 24 h. Fifty μg/mL colchicine, 50 mmol/L 2-deoxyglucose, 50 μg/mL chloroquine, 1 mg/mL ammonium chloride and 6 μg/mL nystatin were added and incubated for 2 h. The C6-PNIPAm solution (diluted with DMEM medium) at a concentration of 300 μg/mL of PNIPAm was added and incubated at 37 ℃ for 2 h in the dark. Next, cells were treated as described above and assessed by use of flow cytometry to study the cellular uptake mechanism.

1.13　Statistical analysis

SPSS 20.0 statistical software was used to analysis da-

ta. The statistical significance of the data was compared by Student's *t*-test.

2 Results

2.1 Optimization of prescription

PNIPAm nanogels were prepared as described in Table 2. Particle size of each sample was observed at three different temperature, including 25 ℃ (room temperature), 37 ℃ (body temperature, which is also higher than the LCST of PNIPAm), 42 ℃ (approximate lethal temperature of tumor cells), respectively. As presented in Figure 2, particle size of PNIPAm nanogel decreased with increasing temperature. These results might be due to the hydrophobic isopropyl and the hydrophilic amide group on the side chain of the PNIPAm nanogel as the amide group enables the synthesized nanogel to undergo volume changes in response to changes in temperature.

As demonstrated in Table 3, variance analysis demonstrated that the concentration of APS (factor B) had a significant effect on the results. As the initiator of the polymerization, the particle size of PNIPAm nanogel increased significantly by increasing APS content from 1% to 5%, which might be attributed to the fact that the polymerization and nucleation rate increased when increasing the concentration of initiator. The polymerization was proceeded fast when the APS was excessive, which might in turn formed nanogel with larger particle size. Concentration of APS (factor B) was identified as a main factor; temperature (factor D), concentration of MBA (factor A) and time (factor C) were secondary factors. Optimal levels were selected for the factors with greatest influence, and other factors that had a lesser influence on results were selected according to their cost, time and benefit. Optimized prescription consisted of $A_3B_1C_1D_2$, which is equal to 8% MBA, 1% APS and a reaction time of 1.5 h at 60 ℃. A prescription equal to $A_3B_1C_1D_2$ did not exist in the orthogonal design; therefore, a supplementary experiment was carried out. As a result, the average particle size obtained at 25 ℃ and 42 ℃ were (70.8±0.91) nm and (44.5±0.46) nm, respectively. The DLS (dynamic light scattering) curve and the transition photograph of PNIPAm aqueous solution at different temperatures (25 ℃ and 42 ℃) were presented in Figure 3. The results indicated that the prescription process of thermo-responsive PNIPAm nanogel was optimized successfully by means of the orthogonal design.

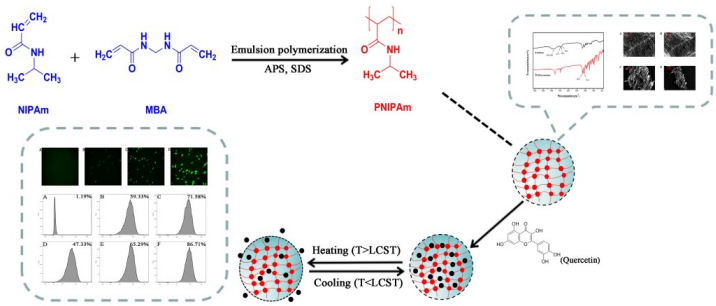

Figure 1　Schematic diagram of PNIPAm and Que-PNIPAm nanogel

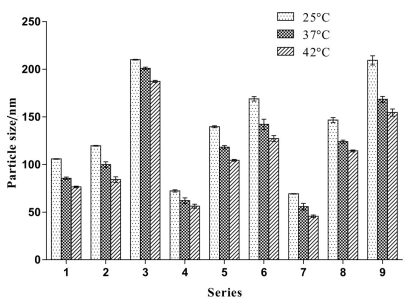

Note: 1 to 9 represent prescriptions at different factors according to the orthogonal design

Figure 2 Particle size of PNIPAm nanogel($\bar{x}\pm s$, $n=3$)

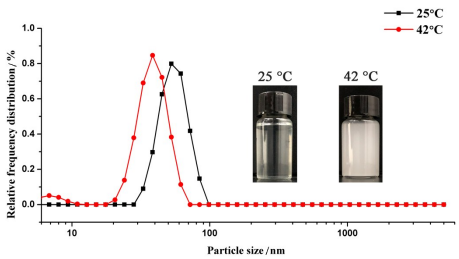

Figure 3 Curve of size distribution and transition photograph of PNIPAm aqueous solution at 25 ℃ and 42 ℃

Table 1　Orthogonal array analysis of PNIPAm nanogel

Levels	Factors			
	A	B	C	D
	MBA /%	APS /%	Time /h	Temperature /℃
1	3	1	1.5	50
2	5	3	2	60
3	8	5	2.5	70

2.2 Fourier transform infrared spectroscopy (FT-IR)

The FT-IR spectra of NIPAm and PNIPAm nanogel were presented in Figure 4. The PNIPAm nanogel had broad absorption bands at 3 100－3 500 cm^{-1}, indicating presence of -NH-. Characteristic bands at 1 620.09 cm^{-1} and 1 545.84 cm^{-1} were observed and correspond to the peaks of vinyl. The peaks of vinyl disappeared at the corresponding position of PNIPAm, indicating that the structure of vinyl in the monomer changed. Absorption peaks at 2 974.98 cm^{-1}, 2 933.53 cm^{-1} and 2 875.67 cm^{-1} were characteristic of C-H absorption peaks of methyl, methylene and methine groups in the main chain of PNIPAm, respectively. Therefore, these results suggested that the NIPAm monomer was polymerized into PNIPAm.

Table 2　Orthogonal design of PNIPAm nanogel($\bar{x}\pm s$)

Series	Factors				Particle size(25℃)/nm
	A MBA/%	B APS/%	C Time/h	D Temperature/℃	
1	3	1	1.5	50	105.9±0.35
2	3	3	2	60	119.7±0.36
3	3	5	2.5	70	210.1±0.38
4	5	1	2	70	72.3±1.15
5	5	3	2.5	60	139.7±1.03
6	5	5	1.5	50	169.0±2.36
7	8	1	2.5	60	69.3±0.31
8	8	3	1.5	70	146.7±2.66
9	8	5	2	50	209.4±4.84
K_1	435.73	247.5	421.57	455.00	
K_2	380.94	406.04	401.4	357.94	
K_3	425.34	588.47	419.04	429.07	
$\bar{K}_1$	145.24	82.50	140.52	151.67	
$\bar{K}_2$	126.98	135.35	133.80	119.31	
$\bar{K}_3$	141.78	196.16	139.68	143.02	
Range	18.26	113.66	6.72	32.36	

Table 3　Variance analysis of PNIPAM nanogel orthogonal design results (25 ℃)

Factors	Sum of square	Degrees of freedom	F	Significance
MBA (%)	563.138	2	7.026	
APS (%)	19 396.835	2	241.992	*
Time	80.155	2	1.000	
Temperature	1 682.607	2	20.992	

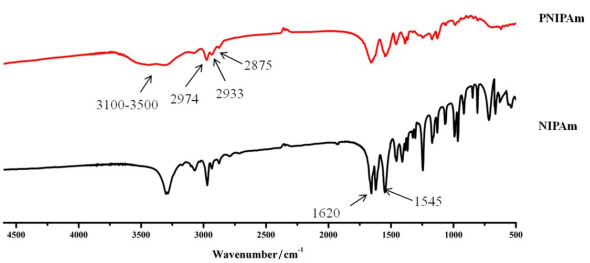

Figure 4　FT-IR spectra of PNIPAm and NIPAm

2.3　Scanning electron microscopy (SEM)

SEM imaging was performed to characterize the morphology of the PNIPAm freeze-dried powders. As presented in Figure 5, the surface of the PNIPAm nanogel had a porous network structure. Thereout, the network could provide drug-loading sites and that drug molecules could be combined with these temperature dependent sites to influence drug release.

2.4　Drug loading

Loading of the Que-PNIPAm nanogel, screened by the single factor experiment, was presented in Figure 6. At the incubation temperatures 4 ℃, 25 ℃ and 37 ℃, drug loading was 0.26%, 0.45% and 2.70%, respectively. The loading capacity of the Que-PNIPAm nanogel was significantly greater at 37 ℃. The rising temperature might strengthen the hydrophobic forces between the PNIPAm chains, thus facilitating bindings of the drug by the polymer. When the ratios of Que and PNIPAm were 1∶5, 1∶10 and 1∶20, drug loading was 0.61%, 1.91% and 2.70%, respectively. Drug loading increased with the increasing amounts of total Que, but the rate of increase decreased, likely due to the limited amount of Que in the polymer. Drug loading was 3.18% when the concentration of PNIPAm was 30 mg/mL. DLS showed that the particle size of Que-PNIPAm was (166.1 ± 2.87) nm (n = 3). The increase in particle size might be attributed to the loading of Que into the PNIPAm nanogel.

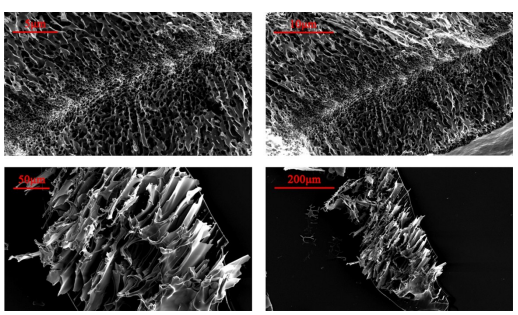

Figure 5　SEM images of PNIPAm nanogel formation at different scales

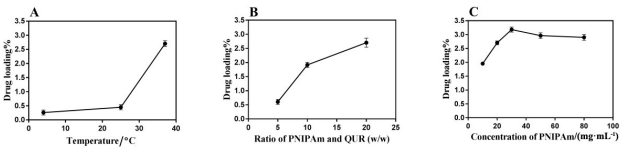

Note: (A) Different incubation temperature. (B) Different ratio of drug and carrier. (C) Different carrier concentration ($\bar{x} \pm s$, $n = 3$)

Figure 6　Drug loading of Que-PNIPAm nanogel

2.5　Transmission electron microscopy (TEM)

As presented in Figure 7, the TEM analysis showed that the Que-PNIPAm nanogel was spherical in shape. In addition, the particle size observed by TEM was slightly smaller than measured by DLS, which might due to the drying process of Que-PNIPAm during TEM sample preparation.

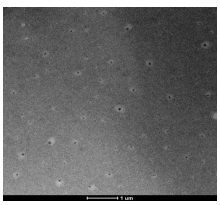

Figure 7　TEM images of Que-PNIPAm nanogel

2.6　*In vitro* drug release

The release profile of Que from PNIPAm were investigated at 37 ℃ and 42 ℃. The cumulative release curve was presented in Figure 8. In the initial period, the released Que from the Que-PNIPAm was only 5.09% (37 ℃) and 6.94% (42 ℃) at 0.25 h, respectively. The maximum rate of release at 37 ℃ was approximately 86.70% and a much higher release of 89.30% was observed at 42 ℃. However, only 6.27% drug was released form Que suspension at 1 h, and about 33.34% of the drug was released at 24 h. Therefore, a significant improvement of the release of Que was observed in a nanogel formulation compared with the Que suspension. The release of Que was increased with the increasing temperature, the higher the temperature the higher the release rate, mainly due to the weakening of hydrogen bond interaction of Que with PNIPAm compared to that at lower temperature where the hydrogen bond interaction was strong enough to hold Que molecules on the PNIPAm.

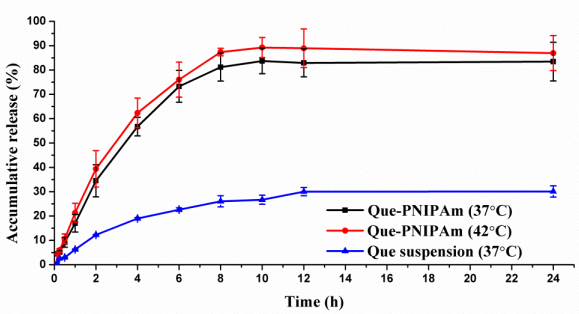

Figure 8　Release profiles of Que from Que-PNIPAm nanogel ($\bar{x} \pm s$, $n = 3$)

2.7　Cytotoxicity

Cytotoxicity of unloaded nanogel, free Que and Que-PNIPAm were investigated using MCF-7 cells. As shown in Figure 9, the unloaded nanogel, at a concentration ranging from 100 to 1 000 μg/mL, had no observable cytotoxicity, this could rule out that the PNIPAm was the cause of cytotoxicity of the Que-PNIPAm. Incubation at 42 ℃ up to 1 h did not significantly affect the viability of MCF-7 cells in the control group. Que-PNIPAm nanogel significantly increased the inhibition rate of MCF-7 cells when compared to cells treated with free Que. As shown in Figure 10, compared to the group treated at 37 ℃, no apparent inhibition was observed in MCF-7 cells treated at 42 ℃ ranging from 1 to 2 μg/mL. However, when raising the concentration of drug to 5 μg/mL or higher, the cell inhibition rate increased significantly. The results were probably because the cellular uptake increased with raised temperature. The rate of inhibition of MCF-7 cells increased with the dose, demonstrating that Que-PNIPAm significantly improve anticancer effects of Que.

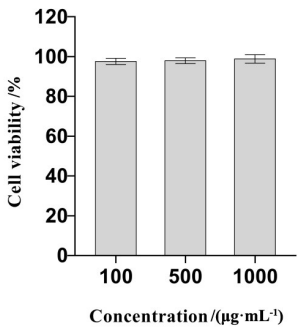

Figure 9　Cell viability of MCF-7 cells for unloaded PNIPAm nanogel ($\bar{x} \pm s$, $n = 3$)

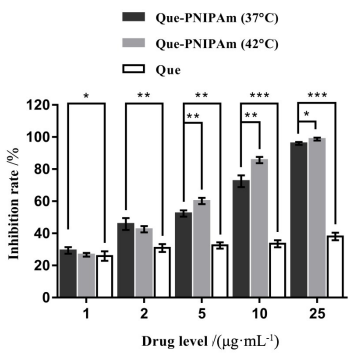

Note: Statistical analysis between different groups was performed using a *one-way* analysis of variance on SPSS 11.0 software. $^{*}P<0.05$, $^{**}P<0.01$, $^{***}P<0.001$.

Figure 10　Inhibitory effect of free Que and Que-PNIPAm nanogel to MCF-7 cells ($\bar{x} \pm s$, $n = 3$)

2.8　Cellular uptake

Cellular uptake studies of Coumarin-6 loaded PNIPAm (C6-PNIPAm) were investigated by visualizing the fluorescence of C6 using fluorescence microscopy. The fluorescence microscopy observations were presented in Figure 11. Cells treated with free C6 solution for 2 h showed almost no fluorescence, indicating that free C6 could not enter MCF-7

cells. However, a bright green fluorescence was observed after 2 h of C6-PNIPAm treatment and the fluorescence increased with increasing concentrations of PNIPAm. In consideration of the similar solubility of C6 and Que, it was evident that drug-loaded PNIPAm nanogel could be easily internalized by MCF-7 cells and cellular uptake was positively associated with drug concentration. The cellular uptake observations at different temperatures were presented in Figure 12, C6-PNIPAm was effectively taken up by MCF-7 cells at 37 ℃, 42 ℃, the fluorescence increased with increasing temperature at equal concentration levels of PNIPAm. It was due to the thermo-responsive properties of the polymer, that the increased temperature led to an enhanced hydrophobic interaction between the polymer and cells.

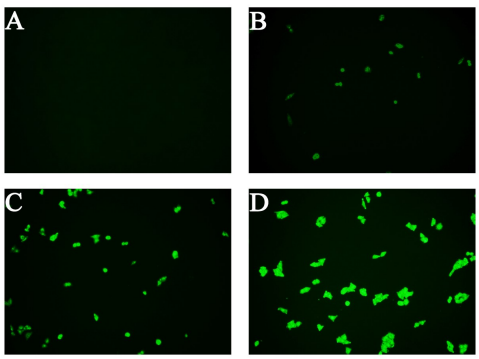

Note: (A) free C6, C6-PNIPAm at different concentration of (B) 75 μg/mL, (C) 150 μg/mL and (D) 300 μg/mL

Figure 11　Fluorescence microscopy images of C6-PNIPAm nanogel in MCF-7 cells for 2 h at 37 ℃

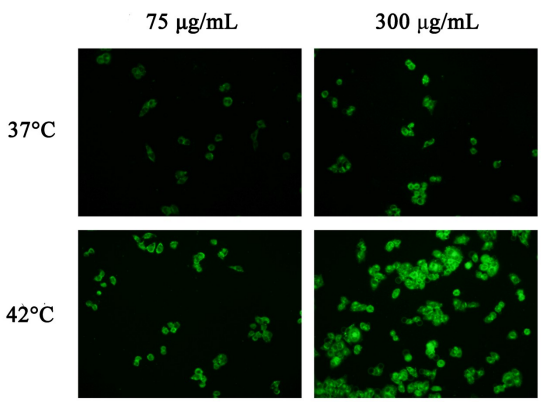

Figure 12　Fluorescence microscopy images of MCF-7 cells exposed to 75 and 300 μg/mL of C6-PNIPAm nanogel for 1 h at 37 ℃ and 42 ℃

The accumulation of C6 in MCF-7 cells at different concentrations and incubation time were presented in Figure 13 using flow cytometry. The percentage of cellular uptake of PNIPAm by the MCF-7 was 1.19%, demonstrating that PNIPAm was hardly uptaken by MCF-7 cells. The percentage of fluorescent cells was 59.33%, 65.29% and 71.58% at the concentration of PNIPAm of 75 μg/mL, 150 μg/mL and 300 μg/mL, respectively. The percentage of fluorescent cells was 47.33%, 65.29% and 86.41% at the incubation time of 1 h, 2 h and 4 h, respectively. These results were consistent with the observations under fluorescence microscope, indicating that cellular uptake increased with increasing concentration and incubation time.

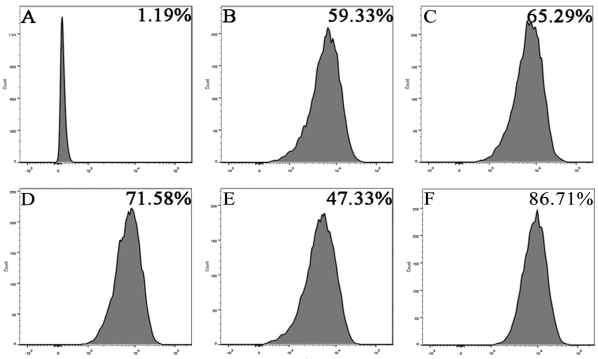

Note: (A) PNIPAm nanogel (unloaded C6) and various C6-PNIPAm for different concentrations and temperatures: (B) 75 μg/mL, (C) 150 μg/mL and (D) 300 μg/mL for 2 h, respectively; (E) 75 μg/mL for 1 h and (F) 75 μg/mL for 4 h

Figure 13 Flow cytometry of C6-PNIPAm nanogel in MCF-7 cells

Various endocytosis inhibitors were used to investigate the mechanism of cellular uptake, namely colchicine (tubulin-mediated inhibitor), nystatin (caveolae-mediated endocytosis inhibitor), 2-deoxyglucose (energy inhibitor), chloroquine (lysosomal inhibitors), and ammonium chloride (lysosomal inhibitors). Results of the studies were presented in Figure 14. When compared with the C6-PNIPAm (without inhibitors added), the percentage of cellular uptake was partially reduced by colchicine (20.54%) and 2-deoxyglucose (12.15%). These results suggested that the uptake of the PNIPAm nanogel by MCF-7 cells was energy-dependent and underwent the tubulin-mediated processes.

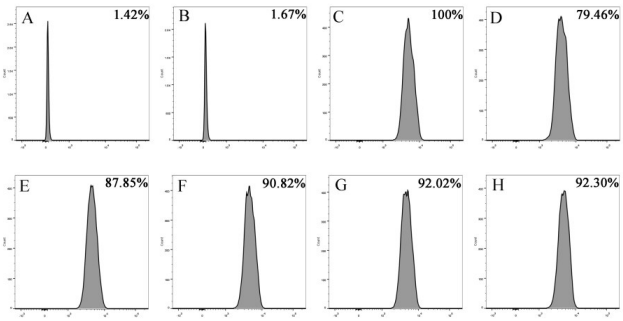

Note: A. blank cells; B. PNIPAm nanogel (unloaded C6); C. C6-PNIPAm and various inhibitors; D. colchicine; E. 2-deoxyglucose; F. chloroquine; G. ammonium chloride and; H. nystatin

Figure 14　Flow cytometry of MCF-7 cells treated with different inhibitors

3　Discussion

To enhance the anticancer efficiency of Que, a thermosensitive PNIPAm nanogel loaded with Que was designed and used in the treatment of MCF-7 breast cancer cells. Firstly, PNIPAm were synthesized and optimized by orthogonal design method. Next, Que was encapsulated in the nanogel with high loading efficiency by simple procedures. The obtained Que-PNIPAm exhibited an accelerated release profile and a thermosensitive property in the *in vitro* release stud-

ies. The cytotoxicity assay indicated that unloaded PNIPAm is non-toxic whereas Que-PNIPAm showed a specific toxicity to MCF-7 cancer cell lines. The internalization of coumarin-6 loaded PNIPAm has been confirmed by fluorescent microscopy. The nanogel exhibited markedly higher cellular uptake to MCF-7 breast cancer cells in the presence of mild hyperthermia. In addition, the uptake of PNIPAm nanogel by MCF-7 cells was energy-dependent and through a tubulin-mediated pathway. Based on the above results, the PNIPAm nanogel represents a promising delivery system to overcome the limitations of hydrophobic drugs such as Que.

References:

[1] KIM MR, LEE JY, LEE HH, et al. Antioxidative effects of quercetin-glycosides isolated from the flower buds of *Tussilago farfara L*[J]. Food Chem Toxicol, 2006, 44 (8): 1299-1307.

[2] WANG XQ, LI GZ, ROW HK. Extraction and determination of quercetin from Ginkgo biloba by DESs-based polymer monolithic cartridge[J]. J Chromatogr Sci, 2017, 55 (8): 866-871.

[3] CHEN ZP, SUN J, CHEN HX, et al. Comparative pharmacokinetics and bioavailability studies of quercetin, kaempferol and isorhamnetin after oral administration of Ginkgo biloba extracts, Ginkgo biloba extract phospholipid complexes and Ginkgo biloba extract solid dispersions in rats[J]. Fitoterapia, 2010, 81 (8): 1045-1052.

[4] YUAN ZP, CHEN LJ, FAN LY, et al. Liposomal quercetin efficiently suppresses growth of solid tumors in murine models[J]. Clin Cancer Res, 2006, 12 (10): 3193-3199.

[5] WU QJ, DENG SY, LI L, et al. Biodegradable polymeric micelle-encapsulated quercetin suppresses tumor growth and metastasis in both transgenic zebrafish and mouse models[J]. Nanoscale, 2013, 5 (24): 12480-12493.

[6] ROGERIO AP, DORA CL, ANDRADE EL, et al. Anti-inflammatory effect of quercetin-loaded microemulsion in the airways allergic inflammatory model in mice[J]. Pharmacol Res, 2010, 61 (4): 288-297.

[7] JIA J, CHEN J. Histone hyperacetylation is involved in the quercetin-induced human leukemia cell death[J]. Pharmazie, 2008, 63 (5):379-383.

[8] PATRA A, SATPATHY S, SHENOY AK, et al. Formulation and evaluation of mixed polymeric micelles of quercetin for treatment of breast, ovarian, and multidrug resistant cancers[J]. Int J Nanomedicine, 2018, 13: 2869-2881.

[9] GAO X, WANG BL, WEI XW, et al. Anticancer effect and mechanism of polymer micelle-encapsulated quercetin on ovarian cancer[J]. Nanoscale, 2012, 4 (22): 7021-7030.

[10] YIN JT, HOU YT, SONG XY, et al. Cholate-modified polymer-lipid hybrid nanoparticles for oral delivery of quercetin to potentiate the anti-leukemic effect[J]. Int J Nanomedicine, 2019, 14: 4045-4047.

[11] MACKIEWICZ M, ROMANSKI J, DROZD E, et al. Nanohydrogel with N,N-bis (acryloyl) cystine crosslinker for high drug loading[J]. Int J Pharm, 2017, 523 (1): 336-42.

[12] SINGH B, KAUR A, DHIMAN S, et al. QbD-enabled development of novel stimuli-responsive gastroretentive systems of acyclovir for improved patient compliance and biopharmaceutical performance[J]. AAPS Pharm Sci Tech, 2016, 17 (2): 454-465.

[13] SIVAKUMARAN D, MAITLAND D, OSZUSTOWICZ T, et al. Tuning drug release from smart microgel-hydrogel composites via cross-linking[J]. J Colloid Interface Sci, 2013, 392: 422-430.

[14] REJINOLD NS, SREEREKHA PR, CHENNAZHI KP, et al. Biocompatible, biodegradable and thermo-sensitive chitosan-g-poly (*N*-isopropylacrylamide) nanocarrier for curcumin drug delivery[J]. Int J Biol Macromol, 2011, 49 (2): 161-172.

[15] YANG HW, LEE AW, HUANG CH, et al. Characterization of poly(*N*-isopropylacrylamide)-nucleobase supramolecular complexes featuring bio-multiple hydrogen bonds[J]. Soft Matter, 2014, 10 (41): 8330-8340.

[16] MALONNE H, EECKMAN F, FONTANIE D, et al. Preparation of poly (*N*-isopropylacrylamide) copolymers and preliminary assessment of their acute and subacute toxicity in mice[J]. Eur J Pharm Biopharm, 2005, 61 (3): 188-194.

[17] XU JJ, PELTON R. A new route to poly(*N*-isopropylacrylamide) microgels supporting a polyvinylamine corona[J]. J Colloid Interface Sci, 2004, 276 (1): 113-117.

[18] MATSUMURA Y, IWAI KJ. Thermo-responsive behavior and microenvironments of poly(*N*-isopropylacrylamide) microgel particles as studied by fluorescent label method[J]. Colloid Interface Sci, 2006, 296 (1): 102-109.

[19] FERNANDES ST, SZARPAK JA, APPAIX F, et al. Thermoresponsive hyaluronic acid nanogels as hydrophobic drug carrier to macrophages[J]. Acta Biomater, 2014, 10 (11): 4750-4758.

[20] CHAI SG, ZHANG JZ, YANG TT, et al. Thermoresponsive microgel decorated with silica nanoparticles in shell: Biomimetic synthesis and drug release application[J]. Colloids and Surfaces A: Physicochem Eng Aspects, 2010, 356 (1): 32-39.

[21] PAN CL, LV HT. Preparative separation of quercetin, ombuin and kaempferide from Gynostemma pentaphyllum by high-speed countercurrent chromatography[J]. J Chromatogr Sci, 2019, 57 (3): 1-7.

[22] QU N, SHI D, SHANG M, et al. Breast cancer cell line phenotype affects sonoporation efficiency under optimal ultrasound microbubble conditions[J]. Med Sci Monit, 2018, 24: 9054-9062.

[23] KUMAR P, WASIM L, CHOPRA M, et al. Co-delivery of vorinostat and etoposide via disulfide cross-linked biodegradable polymeric nanogels: synthesis, characterization, biodegradation, and anticancer activity[J]. AAPS Pharm Sci Tech, 2018, 19 (2): 634-647.

[24] LI LH, ZHAO XB, MA YK, et al. Enhancement of gastrointestinal absorption of quercetin by solid lipid nanoparticles[J]. J Control Release, 2009, 133 (3): 238-244.

[25] BOSE S, MICHNIAK-KOHN B. Preparation and characterization of lipid based nanosystems for topical delivery of quercetin[J]. Eur J Pharm Sci, 2013, 48 (3): 442-452.

[26] SUN M, NIE SF, PAN X, et al. Quercetin-nanostructured lipid carriers: characteristics and anti-breast cancer activities in vitro[J]. Colloids Surf B Biointerfaces, 2014, 113: 15-24.

[27] LI J, LU MJ, JIN J, et al. miR-449a suppresses tamoxifen resistance in human breast cancer cells by targeting ADAM22[J]. Cell Physiol Biochem, 2018, 50 (1): 136-149.

(编辑:董宇)